

J10.5 UAS-based low-altitude freezing precipitation observation system: development updates and initial field deployment results

GUSTAVO B. H. DE AZEVEDO^{a,b}, ALYSSA AVERY^a, DAVID SCHVARTZMAN^{b,c}, BRAYDON REWARD^a, SCOTT LANDOLT^d,
STEPHANIE DiVITO^e, JAMEY D. JACOB^a

^a *Oklahoma Aerospace Institute for Research and Education at the Oklahoma State University*

^b *Advanced Radar Research Center at the University Oklahoma*

^c *School of Meteorology at the University Oklahoma*

^d *Research Applications Laboratory at the National Center for Atmospheric Research*

^e *Federal Aviation Administration*

ABSTRACT: Freezing rain and freezing drizzle can produce nearly undetectable hazards with potentially catastrophic consequences for aircraft within low altitudes (e.g., the terminal area). However, the lack of direct observations of the low-altitude freezing precipitation environment creates a challenge for forecasters, flight crews, dispatchers, and air traffic controllers. This research demonstrates how Unmanned Aerial Vehicles (UAVs) can be designed and instrumented to create Unmanned Aerial Weather Measurement Systems (WxUAS) capable of sampling the low-altitude freezing precipitation environment. This article discusses the initial findings from a small intercomparison study conducted at Marshall Field (CO) during a winter weather event. Additionally, we explore the insights provided by high-resolution thermodynamic and particle size distribution profiles, and its potential contributions to a better understanding of the low-altitude freezing precipitation environment.

1. Introduction

A considerable portion of the negative economic impacts associated with freezing precipitation is produced by shallow, not strongly forced events within the atmosphere's first 1.5 km Tripp et al. (2021). Due to the proximity to the ground and varying range of particle sizes, some of these precipitation phenomena are not well captured by current observation systems (e.g., Radar, ASOS/AWOS, Radiosondes), leading to the underrepresentation of freezing precipitation in forecast models Reeves et al. (2022). In aviation, unpredicted and undetected low-altitude freezing precipitation can produce almost invisible hazards with potentially catastrophic consequences N.T.S.B. (1994). For this reason, in 2015, the Federal Aviation Administration (FAA) introduced a new icing certification rule restricting flights into and out of commercial airports during freezing precipitation to prevent icing-related accidents. Nonetheless, compliance with this rule requires the precise forecast and observation of precipitation type in the lower atmosphere.

In recent years, new tools have been created to integrate data streams from multiple radars, surface and upper air observations, satellites, and forecast models (e.g., HEMS¹, TAIWIN², and MRMS³). However, the coverage and resolution of the current observation systems do not accurately characterize low-altitude freezing precipitation, in particular, freezing rain and freezing drizzle Reeves et al. (2022); Tripp et al. (2021); Tokay et al. (2020); Kurdzo

et al. (2020); Reeves and Waters (2019); Landolt et al. (2019).

Additionally, the lack of direct observations of low-altitude freezing precipitation forces ground and space-based observation systems to rely on inferences or numerically generated atmospheric data to produce their hydrometeor classification outputs Reeves et al. (2022); Hallowell et al. (2013); Park et al. (2009). This dependence reduces the operational reliability of the mentioned data integration tools, leading forecasters, flight crews, dispatchers, and air traffic controllers to rely on human observations (e.g., augmented station and pilot reports). Therefore, there is a need for additional low-altitude freezing precipitation observations to inform and train low-altitude forecast tools. Furthermore, the imminent introduction of small delivery Unmanned Aerial Vehicles (UAVs) and Advanced Air Mobility (AAM) transport vehicles into the National Airspace System (NAS) creates an additional need for high-resolution low-altitude freezing precipitation observations.

To address this critical need, a new Unmanned Aerial Weather Measurement System (WxUAS) is being developed to sample the low-altitude freezing precipitation environment. The WxUAS prototype provides in-situ samples of pressure, temperature, relative humidity, and particle size distribution. It also offers remote samples of hydrometeor reflectivity and Doppler velocity from an onboard, vertically pointing millimeter wave (mmWave) radar. With this sensor payload, the WxUAS characterizes the thermodynamic structure of the lower atmosphere while coupling it with its microphysical properties. Leveraging the mobility of UAVs, the WxUAS creates a spatial distribution of the measured atmospheric parameters. Via repetition of the flight pattern at regular intervals, the WxUAS captures the temporal evolution of the measured parameters'

Corresponding author: Gustavo B. H. de Azevedo, gus@okstate.edu

¹Helicopter Emergency Medical Services (HEMS) tool by the National Weather Service

²Terminal Area Icing Weather Information for the Next Generation Air Transportation System by the FAA

³Multi-Radar Multi-Sensor Tool by the National Severe Storms Laboratory

spatial distribution. These new spatiotemporal measurements within the atmosphere’s first 1.5 km can be used for targeted atmospheric studies, in-situ validation for new models and classification algorithms, and potentially be scaled to bridge the measurements of the current observation systems, increasing flight operations safety.

This article presents the preliminary findings from our first field deployment and shares operational insights gained during the process. Recognizing the intricate design required for the WxUAS to obtain accurate atmospheric samples in active precipitation conditions, we have organized our reporting into two distinct categories: in-situ and remote sampling. This segmentation enables a more in-depth exploration of each payload design aspect. Consequently, this article concentrates on the in-situ sensors of the WxUAS, reserving the presentation of mmWave radar data only as an active precipitation indicator.

2. WxUAS Design

In near 0°C environments, radar reflectivity distributions of rain, snow, freezing rain, ice pellets, drizzle, and freezing drizzle can span a 30 dB range and produce an overlap across scenarios of light, moderate, and heavy precipitation Reeves et al. (2022). Therefore, knowing the atmosphere’s thermodynamic structure is critical for radar-based hydrometeor classification. However, as pointed out by Tripp et al. (2021); Waugh and Schuur (2018), systems such as radiosondes with exposed sensors can be struck by freezing precipitation. Once struck, these systems produce erroneous readings induced by ice-encapsulated sensors.

Additionally, in near-freezing environments, precipitation phase can be affected by temperature variations as small as 0.5°C. Given the heat generated by UAS motors and batteries and the potential atmospheric layer mixing caused by the UAS propellers (in particular in multirotors), sensor placement and sample conditioning are critical for measurement accuracy Greene et al. (2018); Houston and Keeler (2018); Jacob et al. (2018); de Azevedo (2022).

To account for all these requirements, the WxUAS employs a custom-designed sensor housing (fig. 1). This housing is composed of two concentric cylinders. The inner cylinder houses three bead thermistors, two capacitive hygrometers, and one optical particle counter. This housing is actively aspirated at a constant rate (approx. 5 ms^{-1}), and the sensors are symmetrically placed around its perimeter, equidistantly from the center flow. The sensor ring is strategically placed at 2-diameter lengths from the aspiration fan and the inner housing’s intake.

The outer cylinder serves as a passive housing and protects the inner housing from direct contact with precipitation and sunlight. This is possible because the outer housing’s intake extends over the inner housing’s intake and curves downward (see fig. 1, panels “a” and “b”).

Only the inner cylinder housing is aspirated, which will lessen the degree of turbulent heating in the outer cylinder. Additionally, the outer housing’s diameter is twice as large as the inner housing’s diameter. The resultant air gap insulates the sensing section from radiative and sensible heat fluxes and impinging water and snow. Due to its shape, this design can leverage gravity to mechanically separate large precipitation drops from the air. This separation occurs because larger droplets will be dominated by their inertia while small droplets will follow the streamlines on the intake system according to Stokes flow. This flow characteristic allows the system to sample the atmospheric conditions without exposure to harmful freezing precipitation.

The rate of aspiration and interior sensor housing diameter give an approximate Reynolds number of 10,000. This Re number and the two-diameter distance between the sensor section and the inner housing intake ensure the sensors have a consistent flow profile due to well-mixed flow sampled beyond the entrance length (see fig. 1, panels “b” and “c”). The Weber numbers for the objective particles at the flow rate range from 3 - 7. These low spectrum numbers denote the minimal presence of droplets smearing and separating within the inner housing.

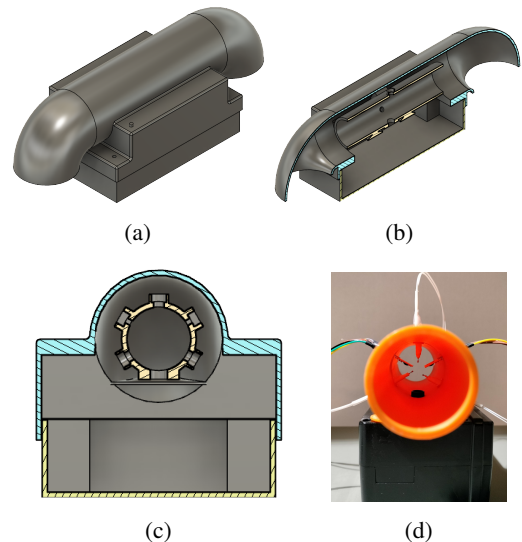


FIG. 1. Two-layer custom sensor housing designed to prevent contact with freezing precipitation while still allowing for direct observation of atmospheric conditions.

The three thermistors and two hygrometers inside the inner housing sample the atmosphere at 10 Hz, while the optical particle counter produces a distribution every second. The higher sampling rate of the thermistors and hygrometers allows for 1-second averaging, which reduces the noise in their outputs. The redundancy and concentric placement strategy for the sensors inside the inner housing

(see fig. 1, panels “c” and “d”) allows us to quality control the data, evaluate flow quality, and increase the system’s precision by reducing the effects of digital quantization.

3. Design Validation

To test the WxUAS’s performance and validate the in-situ sensor housing design, we performed an intercomparison study at Marshall Field, home to the National Center for Atmospheric Research’s (NCAR) Aviation Applications Program. This field station is located on the outskirts of Boulder (CO), 1627 m above sea level (ASL). It has several instrumented towers, a micro rain radar, a distrometer, and a ceilometer, amongst other instruments. This study was done in coordination with the FAA’s TAIWIN team, which provided the low-altitude precipitation forecast that determined our deployment date during a winter weather event in April 2023.

During this winter weather event, the Marshall Field ground-based sensors indicated the presence of drizzle, rain, snow, rain/drizzle, and soft hail at various intensities. They also indicated temperatures between -1 and 2 °C, winds between 0 and 5 ms^{-1} , and cloud bases as low as 80 m above ground level (AGL). These conditions presented an excellent test opportunity, enabling the evaluation of most system features.

The study began with two ground-based experiments to eliminate any potential interference caused by the rotors, creating a control case for the later intercomparison in the Hover flight mode at 10 m (AGL). In these comparison periods, the mean absolute errors were 0.2155 °C and 1.1653 %RH (not shown), and 0.1439 °C and 1.0778 %RH (fig. 2). Both results are below the sensing elements’ accuracies specified by their manufacturers, which are 0.3 °C and 1.8 %RH.

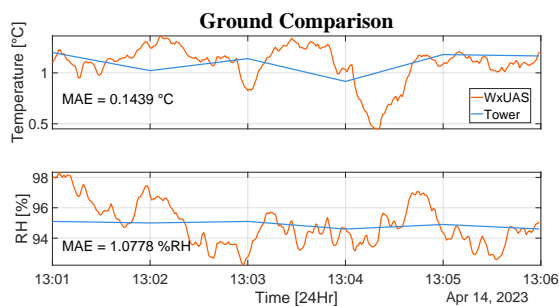


FIG. 2. Results for the second temperature and relative humidity ground-based intercomparison experiment. The small mean absolute errors are below both manufacturers’ reported accuracies.

During these same ground-based experiments, the Marshall Field distrometer reported snow with total counts increasing from 0 to 400 particles per minute. During

this same period, the WxUAS’s 77 GHz vertically pointing radar detected a 15 to 25 dB increase in reflectivity with Doppler velocities of -2 and -4 ms^{-1} . In this same period, the optical particle counter inside the in-situ sensor housing did not report any change in particle size distribution.

These results are shown in fig. 3, where the left panel presents the temporal evolution of the particle size distribution’s mode, and the right panel presents three “Doppler vs. Range” plots. Evaluating the particle size distribution’s mode, it is possible to note the distribution’s bin with the highest count remained between 0 and 2 μm with a total count between 50 to 100 particles per second. These rates and distribution modes are consistent with the sensor’s background readings.

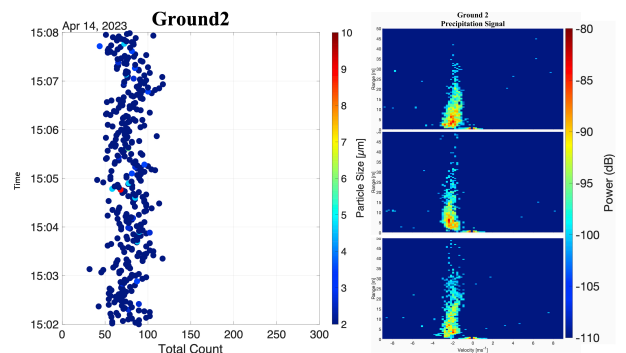


FIG. 3. Results for particle size distribution and reflectivity and Doppler velocity during the second ground-based experiment. For the vertically pointing radar, negative Doppler velocities indicate particles falling towards the radar.

The results from these ground experiments reveal that, during active precipitation, the sensor housing design effectively utilized gravity to mechanically separate large precipitation from the air, avoiding impinging the system’s sensing elements. Additionally, the small mean absolute errors in temperature and relative humidity indicate the design strategy does not introduce any bias or artifacts. Combined, these results validate the in-situ sensor housing design and confirm our expectations regarding the mechanical separation of large precipitation drops from the air while eliminating the impact of radiative and sensible heat fluxes.

4. Initial Results

Upon conclusion of the ground-based and hover experiments, we performed four vertical profiles from the ground to 120 m to evaluate the WxUAS’s ability to characterize the atmosphere’s thermodynamic structure and its micro-physical properties in near-freezing conditions. Although the WxUAS was designed to perform profiles up to 1500 m, we had to limit our flight ceiling for compliance with the FAA’s Part 107 rules. This limitation was unfortunate as it

could have hindered our ability to observe any meaningful structural change with height. However, given our proximity to the mountains, the flight field's elevation (1627 m, ASL), and the intensity of the weather event, our four profiles were performed in scientifically relevant conditions and permitted us to gauge the WxUAS's potential.

Our initial results are presented below, where fig. 4 depicts the WxUAS temperature and relative humidity profiles (indicated by red lines) juxtaposed with the tower sensors' at 2 m (represented by blue dots), and fig. 5, displays the particle size distribution profiles (bottom panels) against the ground-based ceilometer data (top panels). In all plots, the y-axis signifies altitude, and the x-axis corresponds to the variable of interest. For the particle size distribution profiles, the data represents the distribution's mode – the particle size bin with the highest count. The color in these profiles denotes the mode's particle size, while the x-axis portrays the distribution's total count for that second. For the ceilometer scatter plot, the orange shaded columns represent the time intervals for the four flights.

The first profile occurred immediately after an intense snow event had subsided, while the ceilometer reported a low-altitude cloud base near 95 m AGL (fig. 5). The snow, freshly deposited on the ground, produced lower temperatures and intense moisture on the surface layer, as reported by the tower instruments (the blue dots on fig. 4). These conditions were also reflected in the WxUAS measurements. Most notably in the particle counter data that showed distribution modes with total counts above 150 particles per second on the surface, falling to 100 between 10 and 50 m AGL and rising to 200 between 80 to 110 m (fig. 5: 'Mission 1').

The high count of smaller particles (from 0 to 4 μm) near the ground is most likely produced by the rotor wash during takeoff over the snow-covered surface. While other effects could yield similar increases in small particle count, the likelihood of rotor wash effects is substantiated by the similar pattern observed during 'Mission 4' following a drizzle event. Additionally, this pattern is notably absent in 'Mission 2' and 'Mission 3' after periods without precipitation and during the ground-based intercomparison experiments (fig. 3), which were conducted during a snowfall event with the rotors turned off. The high count of larger particles (from 8 to 11 μm) from 80 to 110 m shows agreement with the ceilometer's reported cloud base, which had a median altitude of 95.5 m, interquartile range (IQR) of 18 m (between [91 109]), and 82 to 118 m minimum and maximum values. This result demonstrates the system's ability to detect cloud-sized particles and characterize the cloud layer's depth.

Furthermore, upon comparing the four particle size distribution profiles with the ceilometer reports, the WxUAS's high sensitivity to cloud-sized particles becomes evident. During the interval between 'Mission 1' and 'Mission 3,'

as the reported cloud base ascended from 95 to 400 m and subsequently descended in 'Mission 4' and beyond, the distribution mode profiles identified by the WxUAS began to manifest the size variation with altitude consistent with the ceilometer reports, albeit earlier. For instance, during 'Mission 3', the reported cloud base exhibits a median altitude of 411 m with an IQR of 305 m. Concurrently, the size distribution profile reveals an increase in particle sizes above 80 m. During 'Mission 4', the reported cloud base, characterized by a median altitude of 384 m and an IQR of 37 m, corresponds to an increase in particle sizes above 60 m, with particles reaching 11 μm at 120 m. Approximately 40 minutes after 'Mission 4', the ceilometer reports the cloud base at 137 m with an IQR of 91 m. Subsequently, one hour later, the ceilometer records the cloud base at 82 m with a 27 m IQR, between 73 and 100 m.

Another illustration of the WxUAS's sensitivity is evident in the profiles gathered during 'Mission 3'. While the temperature and relative humidity profiles from the remaining flights indicate a warmer surface layer cooling above 10 m AGL (as depicted in fig. 4), accompanied by marginal decreases in relative humidity with altitude, 'Mission 3' stands as an exception to this pattern. This particular mission unfolded 26 minutes after civil twilight amid a drizzle event. In this unique scenario, the WxUAS profile reveals an elevation in relative humidity with height and a pronounced temperature drop, reaching freezing temperatures above 15 m AGL. This outcome underscores the WxUAS's potential role in identifying hazardous situations, particularly when ground-based sensors fail to report freezing precipitation events.

5. Discussion

This article introduces a novel Unmanned Aerial Weather Measurement System designed for sampling the low-altitude freezing precipitation environment. Consequently, it is important to present at least a brief discussion on the operational aspects of WxUAS measurements, especially concerning the challenges posed by near-freezing temperatures.

Rotor wash – Although UAV-based sampling systems leverage their mobility for high-resolution atmospheric measurements, they can also present some limitations near the surface. For example, the layer mixing induced by rotor wash in multi-rotor vehicles can produce data artifacts below 10 m as shown by the particle size distributions for 'Mission 1' and 'Mission 4'. In both cases, precipitation on the ground seemed to induce a higher particle count. Therefore, in cases where features near the ground are important, vehicles should be designed for low rotor wash, and their limitation should be properly characterized. For this reason, the sampling technology presented here was developed via an integration into the flight controller.

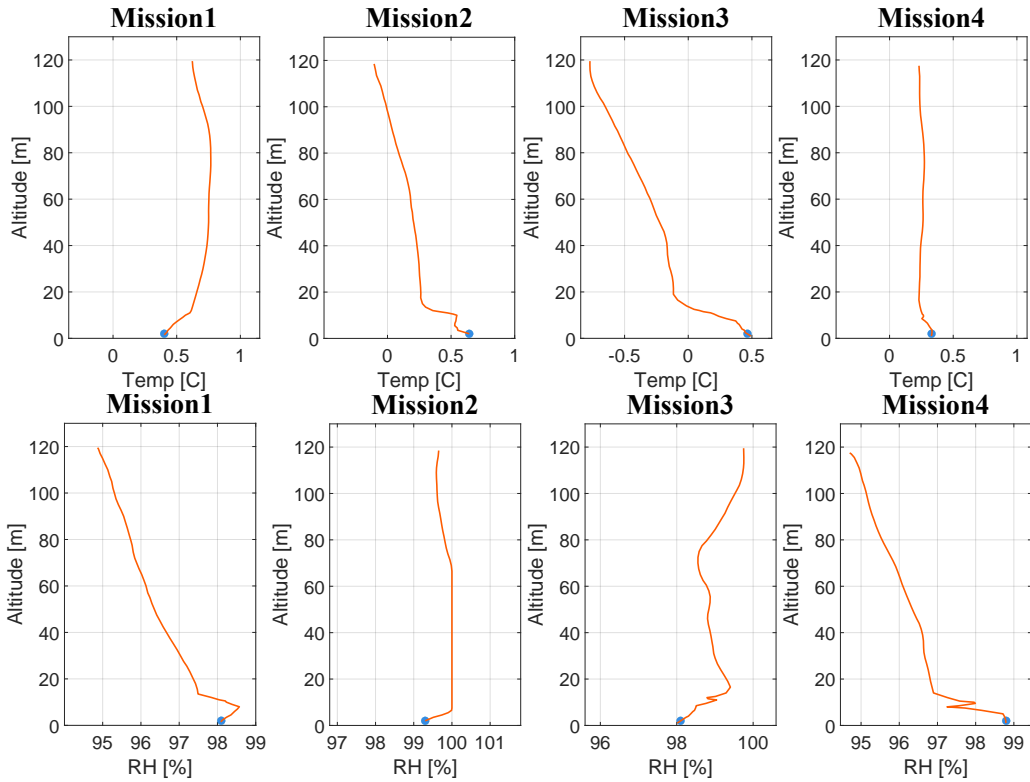


Fig. 4. Temperature and Relative Humidity profiles across the four flights to 120 m above ground level.

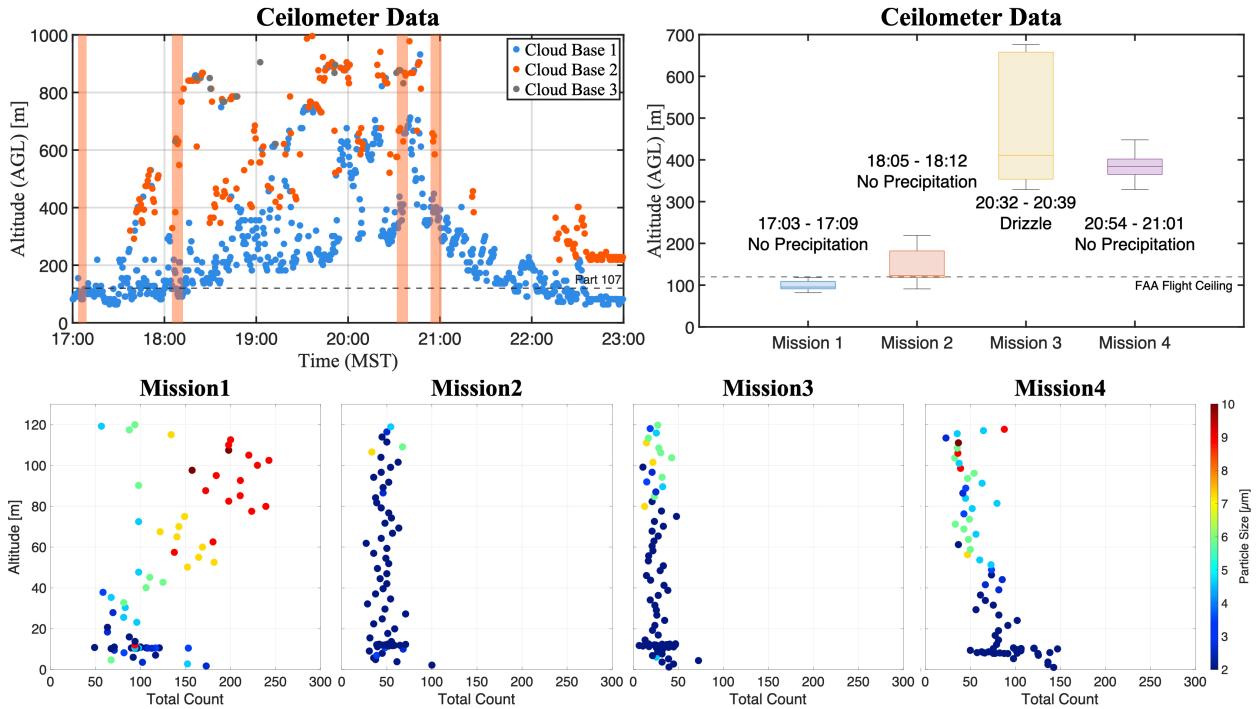


Fig. 5. Ceilometer data (above) indicating the cloud base, and profile of particle size distribution (below) for each of the four flights to 120 m. The orange-shaded columns in the ceilometer's scatter plot represent the time intervals for the four flights

Besides eliminating redundancies in the sampling system, this integration makes the presented solution platform agnostic and multi-modal (i.e., for fixed or rotary-wing UAVs).

Sensor equilibrium – Some UAS components require additional care in near-freezing environments (e.g., the flight controller, batteries, propellers, and the humans monitoring the system). For this reason, keeping the vehicle in a heated environment between flights may be necessary. Unfortunately, keeping the aircraft warm also means warming the sensors. Therefore, it is essential to allow the sensors to reach equilibrium with the environment before starting a new profile. The time required for sensors to reach equilibrium with the sampling environment depends on the temperature difference between the sensors and the environment, the sensor aspiration rate, and the total system time response.

Low altitude forecast – Our field deployment was strategically guided by the forecast expertise of the FAA’s TAI-WIN team, complemented by the support of meteorologists from NCAR’s Aviation Applications Program. Their precise forecasting efforts positioned us amidst a winter weather event characterized by various precipitation types, enabling testing and validation of the WxUAS. However, it is crucial to highlight that even these seasoned experts encountered limitations in the available tools for providing low-altitude hourly forecasts to guide our flights. Notably, in the case of ‘Mission 3’, the preparation to fly and sample drizzle was triggered by a human observer who reported the incoming weather from a strategic vantage point. These limitations further highlight the importance of novel technology to support their work.

Flight restrictions – Low-altitude freezing precipitation poses a significant yet largely undetected and unforecasted hazard for manned and unmanned aircraft. To conduct an effective study of this environment that accounts for the precipitation phase changes between the generation and the surface layers, comprehensive sampling across the entire airspace between them is essential. Achieving this may require the systems to sample from the surface to 2000 m, potentially even penetrating cloud layers. However, existing regulations imposed by the FAA restrict these operations for UAS due to associated risks.

For this intercomparison study, we partnered with the Rocky Mountain Metropolitan Airport (KBJC) and Vigilant Aerospace to submit an altitude and cloud restriction waiver request. In our proposed setup, we would fly up to 600 m inside the KBJC’s class D airspace, under tower control, and would deploy Vigilant Aerospace’s Flight Horizon System as a redundant electronic detect and avoid system. The flight Horizon System employs a ground-based radar and ADS-B receiver to project potential collision trajectories for cooperative and non-cooperative aircraft and provides the Remote Pilot In Command (RPIC) with an avoidance maneuver prescription.

Considering the nature of winter weather research, our flights were planned to occur in conditions typically outside the operating capabilities of most non-commercial aircraft, thereby minimizing the risk of airspace conflict. Regrettably, despite our efforts to design a low-risk experimental setup, the FAA did not deem it safe enough, leading to the denial of our waiver request. Nonetheless, the need for this type of research and the characterization of low-altitude freezing precipitation remains. Therefore, in the absence of a regulatory path for this type of research, the safe sustainment of current operations and the introduction of the next generation of low-altitude aircraft (e.g., small Unmanned Aerial Vehicles and Advanced Air Mobility aircraft) in the National Airspace System will likely remain difficult.

6. Conclusion

The data presented in this article aims to offer a snapshot of the system’s current developmental stage, creating an avenue for early feedback from the winter weather and aviation weather communities. Nevertheless, the provided results showcase crucial validations of key features. Most notably, the sensor housing design exhibits the capability to utilize gravity for the mechanical separation of large precipitation from the air. This functionality prevents the impingement of the system’s sensing elements while ensuring the reduction of bias or artifacts in the data. Additionally, the particle size distribution profiles demonstrated the system’s high sensitivity to the smaller cloud-sized particles.

Details on the airborne 77 GHz radar’s performance and further development updates will be expounded upon in a complementary article. Nevertheless, the results presented in this article illustrate the WxUAS’s potential to characterize the lower atmosphere’s thermodynamic structure in freezing precipitation environments while coupling it with its microphysical properties.

Acknowledgments. The authors thank and acknowledge Bill Doyle from Momentum Drones for his contributions to the sensor payload parts manufacturing; Daniel Tripp from OU-CIWRO for his insights into the modeling and general aspects of the freezing precipitation environment; David Grimsley from the Oklahoma Mesonet for his assistance in calibrating the temperature and humidity sensors; and Kraettli Epperson from Vigilant Aerospace for his partnership in developing a safer concept of operations for WxUAS in clouds. This research was funded in part by the NASA University Leadership Initiative WINDMAP under award 80NSSC20M0162 and by the OAR UxS Research Transition Office with the National Weather Service, “Enabling Research to Operations of sUAS for Improved Weather Forecasting”.

Data availability statement. The data for the Marshall Field intercomparison study is available at

“<https://zenodo.org/doi/10.5281/zenodo.10553162>”. For more information, please contact the corresponding author.

References

- Britto Hupsel de Azevedo, G., B. Doyle, C. A. Fiebrich, and D. Schwartzman, 2022: Low-complexity methods to mitigate the impact of environmental variables on low-cost uas-based atmospheric carbon dioxide measurements. *Atmospheric Measurement Techniques*, **15** (19), 5599–5618, <https://doi.org/10.5194/amt-15-5599-2022>.
- Greene, B. R., A. R. Segales, S. Waugh, S. Duthoit, and P. B. Chilson, 2018: Considerations for temperature sensor placement on rotary-wing unmanned aircraft systems. *Atmospheric Measurement Techniques*, **11** (10), 5519–5530, <https://doi.org/10.5194/amt-11-5519-2018>.
- Hallowell, R. G., M. F. Donovan, D. J. Smalley, and B. J. Bennett, 2013: Icing hazard detection with nexrad ihl. *36th Conf. on Radar Meteorology*.
- Houston, A. L., and J. M. Keeler, 2018: The impact of sensor response and airspeed on the representation of the convective boundary layer and airmass boundaries by small unmanned aircraft systems. *Journal of Atmospheric and Oceanic Technology*, **35** (8), 1687 – 1699, <https://doi.org/10.1175/JTECH-D-18-0019.1>.
- Jacob, J. D., P. B. Chilson, A. L. Houston, and S. W. Smith, 2018: Considerations for atmospheric measurements with small unmanned aircraft systems. *Atmosphere*, **9** (7), <https://doi.org/10.3390/atmos9070252>.
- Kurdzo, J. M., E. F. Joback, P.-E. Kirstetter, and J. Y. N. Cho, 2020: Geospatial qpe accuracy dependence on weather radar network configurations. *Journal of Applied Meteorology and Climatology*, **59** (11), 1773 – 1792, <https://doi.org/https://doi.org/10.1175/JAMC-D-19-0164.1>.
- Landolt, S. D., J. S. Lave, D. Jacobson, A. Gaydos, S. DiVito, and D. Porter, 2019: The impacts of automation on present weather-type observing capabilities across the conterminous united states. *Journal of Applied Meteorology and Climatology*, **58** (12), 2699 – 2715, <https://doi.org/https://doi.org/10.1175/JAMC-D-19-0170.1>.
- National Transportation Safety Board, 1994: In-flight icing encounter and loss of controll: Simmons airlines, d.b.a. american eagle 4184. *Aircraft Accident Reports*.
- Park, H. S., A. V. Ryzhkov, D. S. Zrnica, and K.-E. Kim, 2009: The hydrometeor classification algorithm for the polarimetric wrs-88d: Description and application to an mcs. *Weather and Forecasting*, **24** (3), 730 – 748, <https://doi.org/https://doi.org/10.1175/2008WAF2222205.1>.
- Reeves, H. D., N. Lis, G. Zhang, and A. A. Rosenow, 2022: Development and testing of an advanced hydrometeor-phase algorithm to meet emerging needs in the aviation sector. *Journal of Applied Meteorology and Climatology*, **61** (5), 521 – 536, <https://doi.org/10.1175/JAMC-D-21-0151.1>.
- Reeves, H. D., and J. Waters, 2019: Dual-polarized radar coverage in terminal airspaces and its effect on interpretation of winter weather signatures: Current capabilities and future recommendations. *Journal of Applied Meteorology and Climatology*, **58** (1), 165 – 183, <https://doi.org/10.1175/JAMC-D-18-0123.1>.
- Tokay, A., L. P. D’Adderio, D. B. Wolff, and W. A. Petersen, 2020: Development and evaluation of the raindrop size distribution parameters for the nasa global precipitation measurement mission ground validation program. *Journal of Atmospheric and Oceanic Technology*, **37** (1), 115 – 128, <https://doi.org/10.1175/JTECH-D-18-0071.1>.
- Tripp, D. D., E. R. Martin, and H. D. Reeves, 2021: Applications of uncrewed aerial vehicles (uavs) in winter precipitation-type forecasts. *Journal of Applied Meteorology and Climatology*, **60** (3), 361 – 375, <https://doi.org/10.1175/JAMC-D-20-0047.1>.
- Waugh, S., and T. J. Schuur, 2018: On the use of radiosondes in freezing precipitation. *Journal of Atmospheric and Oceanic Technology*, **35** (3), 459 – 472, <https://doi.org/https://doi.org/10.1175/JTECH-D-17-0074.1>.